V.Epshteyn (ITEP (Moscow) 9 June 2004, Draft 0 (unfinished, not for distribution)
Updates: 22 June 2004, with P.Gorbunov (Univ. of Toronto and ITEP)

MC simulation of the FCAL performance and a comparison with TB'2003 results[1]

In this note the FCAL characteristics experimentally observed in electron and pion beams in the 2003 tests are confronted with MC simulations. The note is incomplete: only electrons are covered so far. The pion simulation and the analysis are in progress.

1. Simulation model includes:

- the beam particle absorption in the calorimeter is simulated with GEANT3.21 (ATLAS version with ATLSIM extensions);
- a conversion of the energy absorbed in liquid argon into ion-electron pairs;
- a drift of electrons in liquid argon;
- a formation of the current signal in individual tubes;
- a formation of an output signal from the groups of tubes;
- the electronic noise;
- the amplifier-shaper;
- sampling of the shaped signal with the FADC.

In the case of a full simulation, the output data are formatted into a stream similar to the Fcal'2003 raw data and the same analysis software is used to analyze real and simulated data. For the FEB signal reconstruction (fit) in each event, the waveform shapes from the FCAL electronics simulation are used. For convenience of the comparison of real and MC data, the transformation factor of the electronic channel is chosen so as to get the average signal amplitude of 1160 ADC counts for 100 GeV electrons − approximately the same as for real electrons.

As will be discussed below, a partial simulation of the energy absorption and the noise was also performed to investigate contributions of the separate components of the model. In that case, obviously, no convertion to the raw data format was done.

The geometry and beam parameters

The FCAL 1, 2 and 3 modules were described in the Geant 3.21 model as 45 cm deep blocks with the square cross-section of 50×50 cm², see Fig. 1. The auxiliary elements like the tubes and spacers were neglected. This simplification (compared to the standard ATLSIM geometry) helped to speed-up the simulation, without any loss in the physics outcome − at least for electrons hitting the area with a regular tube structure. That the influence of the auxiliary elements could be neglected, was shown in a separate study conducted before starting a mass MC production.

The beam impact point was uniformly spread over the $|X|\le3.5$cm, $|Y|\le3.5$cm. An additional data set was produced with a fixed impact point at X=Y=0 (the center of a rod). The slope of the beam particles was about the same as in TB 2003 exposures: $\theta=4.3^{o}$ ($Pz=P0*\cos(\theta)$, $Px=P0*\sin(\theta)$, $Py=0$).

No material in front of the calorimeters was simulated.

[1] A tentative title.

2. The results for electrons

As was discussed in earlier analysis notes [1], to reconstruct the energy of electron-induced events − both in real and MC data – the signals are summed up from the tubes whose centers fall into the circle with the radius *r_core* centered at the particle impact point[2]. Starting from *r_core*=8 cm, the response and the resolution, both for data and MC, do not depend on *r_core.* All the results below are quoted for *r_core* = 8 cm.

- **Sampling fraction** – a fraction of the energy deposited in the active liquid argon gaps – 1.39%.
- **Current-unit calibration for the FCAL1** – the correspondence between the amplitude of the total current in the tubes and the incoming particle energy – 1.7μA/GeV (for the ion-electron pair production energy of 25 eV/pair).
- **The response** depends linearly on the incoming particle energy. However, unlike with real data [1,2], there is no offset in the MC results. This can be related to the absence of a simulated dead material in front of the FCAL and to the way of processing of very small signals. A further study is required.
- **"Measured" energy distributions for MC** are shown in Fig. 1.1. As the electron energy increases, one observes an increasing deviation of these distributions from the Gaussian shape: the right tail gets longer and the left tail shorter. The same behavior is seen in the experimental data. What causes this effect? When analyzing the real data [1], we suggested that this could be related to the electronic noise. Since it was impossible to exclude the noise from data, we were adding *extra* noise by hand, which resulted in *decreasin*g the distribution asymmetry. This indirectly supported our hypothesis on the randomizing effect of the noise.

  In MC we could turn the noise off entirely and see that without it, the deviation from the Gaussian shape persists at all energies, Fig. 1.2. Therefore, this effect is a property of the absorbed energy fluctuations. At low energies, when the noise contribution is greater or comparable with the absorbed energy fluctuations, the effect of the latter is masked out.

  To understand the origin of the intrisic deviation from the Gaussian, one can look at the simulated measured energy distribution for a fixed beam impact point X=Y=0, without noise (Fig. 1.3). It is much closer to the Gaussian that for a smeared beam. The same plots also demonstrate the dependence on the impact point co-ordinates. When the beam is smeared over the calorimeter area, the resulting energy distribution consists of individual partial distributions with different means and develops the observed shape distortion. We note that the FCAL1 response averaged over the area |X, Y|≤3.5cm is *greater* than the response for the fixed impact point X=Y=0.

  Thus, we conclude that the main cause of the non-Gaussian shape of the measured energy distributions is the non-uniform structure of the calorimeter.

---

2 It is implicitly assumed that in the case of real data the impact point can be accurately measured with the beam trackers.

Table 1. Parameters **a**, **b**, **c** of the energy resolution formula, for electrons.

№	condition	a, %	b, %(√GeV)	c, %(GeV)
1	Model, noise off, X=0, Y=0	1.08±0.13	20.3±0.2	-
2	Model, noise off, |X, Y|≤3.5cm, Efluct_only	3.92±0.11	21.6±0.4	-
3	Model, noise off, |X, Y|≤3.5cm	3.96±0.10	22.5±0.4	-
4	Model, noise on, |X, Y|≤3.5cm, Efluct _only	3.70±0.22	24.6±3.9	141±5.4
5	**Model, noise on, |X, Y|≤3.5cm**	**3.67±0.26**	**23.9±3.8**	**140±6.3**
6	Model, noise on, |X, Y|≤3.5cm, Efluct _only, E_Gaussian	3.92±0.08	21.2±1.3	140±3.3
7	Model, noise on, |X, Y|≤3.5cm, E_Gaussian	3.94±0.08	21.8±1.3	139±2.7
8	**Test 2003 data**	**3.76±0.06**	**24.5±0.8**	**145±1.6**

Notes:

Efluct _only – only fluctuations of the energy absorbed in the active Lar gaps are taken into account. By default, the GEANT simulation is used, unless the "E_Gaussian" option is selected. The subsequent signal formation and digitization are not simulated.

E_Gaussian – the energy deposited in the active Lar gaps is modelled by a Gaussian distribution *G(R(E), σ(E)),* where *R(E)* and *σ(E)* are the average response and the resolution computed with the "Efluct_only, noise off " options for the beam energy *E*. The purpose of this mode is explained in the text.

noise on/off – the electronics noise is simulated (on) or not (off).

- **The energy resolution.** Fig. 1.4 shows a good agreement of the model with the experimental data. Let us take a closer look at the calorimeter resolution and the parameters ***a, b, c*** of the resolution curve $\frac{\sigma(E)}{E} = a \oplus \frac{b}{\sqrt{E}} \oplus \frac{c}{E}$ (Fig. 1.5 and Table 1). The parameters found from the full simulation and from the real data (lines 5 and 8 of the Table 1) agree within the statistical errors.

The constant term ***a*** is different from zero even if the particle hits the fixed point in FCAL1 (for X=Y=0, ***a***≈1%). With |X, Y|≤3.5 cm, the constant term increases to ≈3.7%, for the reasons discussed earlier. For an additional illustration, see Fig. 1.6 showing a simulated response as function of the impact point X- and Y co-ordinates. The response is modulated along Y and is flat in X. A similar behavior is observed in real data (see Figures 10, 11 of [1] and the explanations therein).

The stochastic term ***b*** slightly increases (from 20% to 22%, lines 1 and 3 of Table 1) when switching from a “pin” beam (X=Y=0) to a diffused beam |X, Y|≤3.5 cm − again, because of the dependence of the response on the impact point position... [commentaries]. Fig. 1.5 shows that there is no energy domain where the stochastic term clearly dominates. Its influence is noticeable only in the narrow energy range of (30-60) GeV. At lower energies the resolution is dominated by the noise term, at higher energies − by the constant term. As a consequence, the estimation of the stochastic term from the resolution curve is not robust: it can be expected to be very sensitive to statistical uncertainties in σ/E determined within the full energy range.

Indeed, adding the electronic noise to the simulation model leads to a sharp increase of the error of ***b*** (lines 3 and 5 of Table 1). With such big errors it is hard to say anything on a possible influence of the electronic noise on this parameter. The GEANT statistics needs to be increased by an order of magnitude, which is currently impossible due to limited CPU resources.

However, if we wish to assess the effect of all factors beyond the energy absorption in the calorimeter and the noise – the electronics, digitization, signal shape reconstruction etc – a simplified MC model without GEANT, assuming a purely Gaussian absorbed energy spread, can be employed. In that case, we can easily multiply the statistics. We see (lines 6 and 7 of Table 1) that the effect, if any, is very small (a few percent of ***b*** value). We also note that, expectedly, neither ***a***, nor ***c*** are sensitive to the “post-noise” contributions.

The conclusions: for electrons, we have a fairly good agreement between predictions of the GEANT 3.21-based model and the behavior of the real FCAL. However, to reduce the errors of the predicted stochastic term, a dramatic increase of the MC statistics is required. The origin of the observed FCAL response offset (in particular, the rôle of the material in the beam line) has to be separately studied.

References

1. V.Epshteyn, P.Shatalov and P.Gorbunov, *The analysis status report,* ATLAS-FCAL Internal Note 4, 2003-10-30 (http://cern.ch/atlas-fcaltb/Memos/Analysis/ITEP_note4).
2. V.Epshteyn, P.Shatalov and P.Gorbunov, *The analysis status report,* ATLAS-FCAL Internal Note 6, 2004-02-06 (http://cern.ch/atlas-fcaltb/Memos/Analysis/ITEP_note6).

Figures

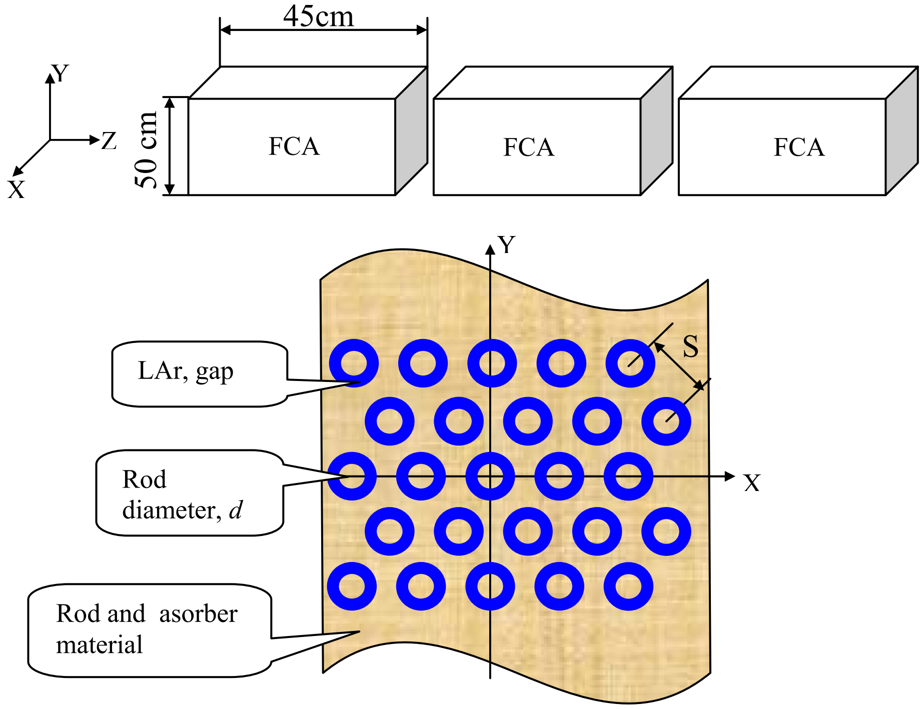

	Absorber material	rod d, mm	LAr gap, mm	S, mm
FCAL1	copper	4.71	0.27	7.500
FCAL2	tungsten	4.93	0.375	8.179
FCAL3	tungsten	5.50	0.500	9.000

Figure 1: FCAL geometry model in GEANT.

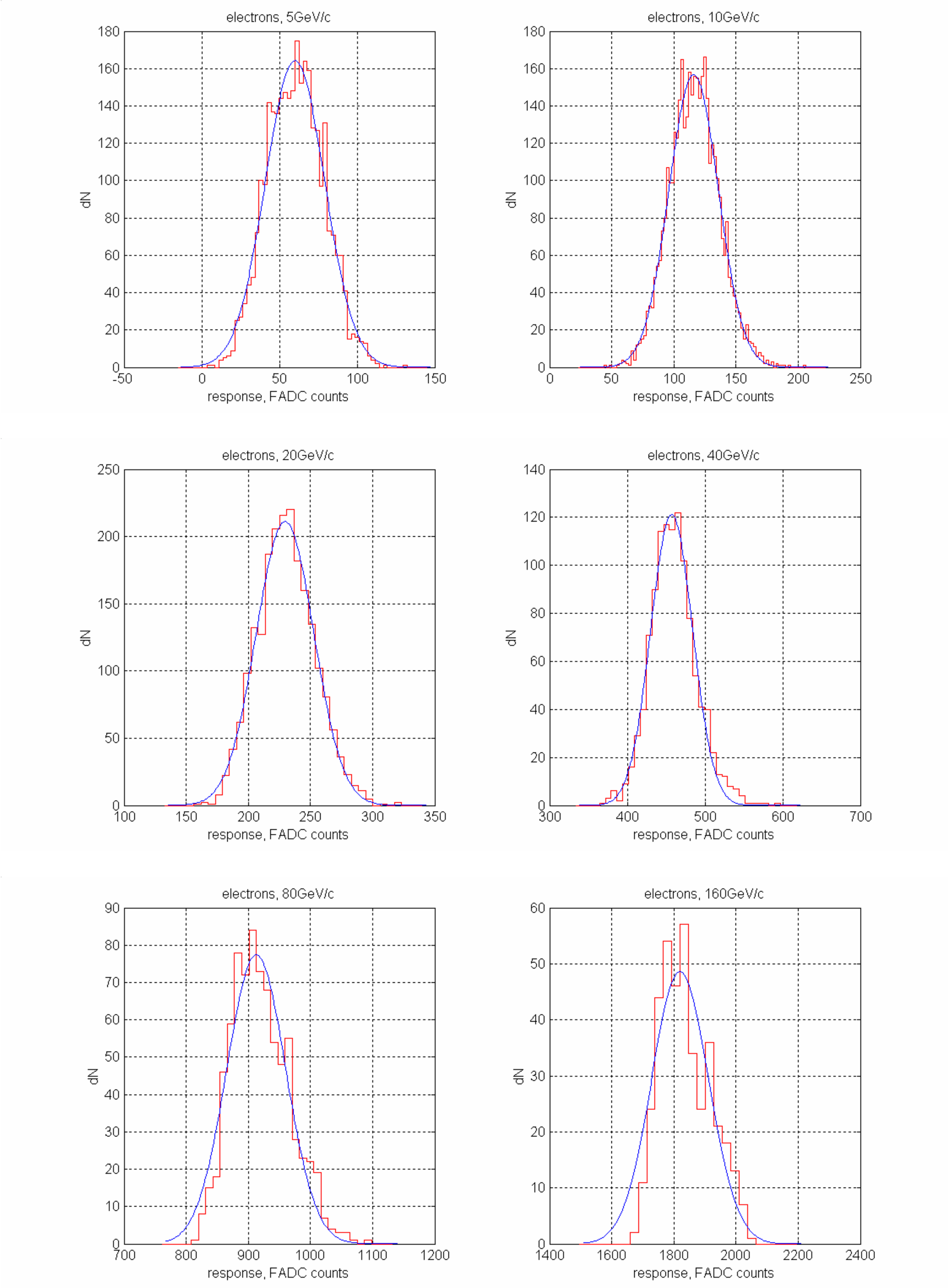

Figure 1.1: Distributions of the total signal in FCAL1: —— model data, —— Gaussian fit.

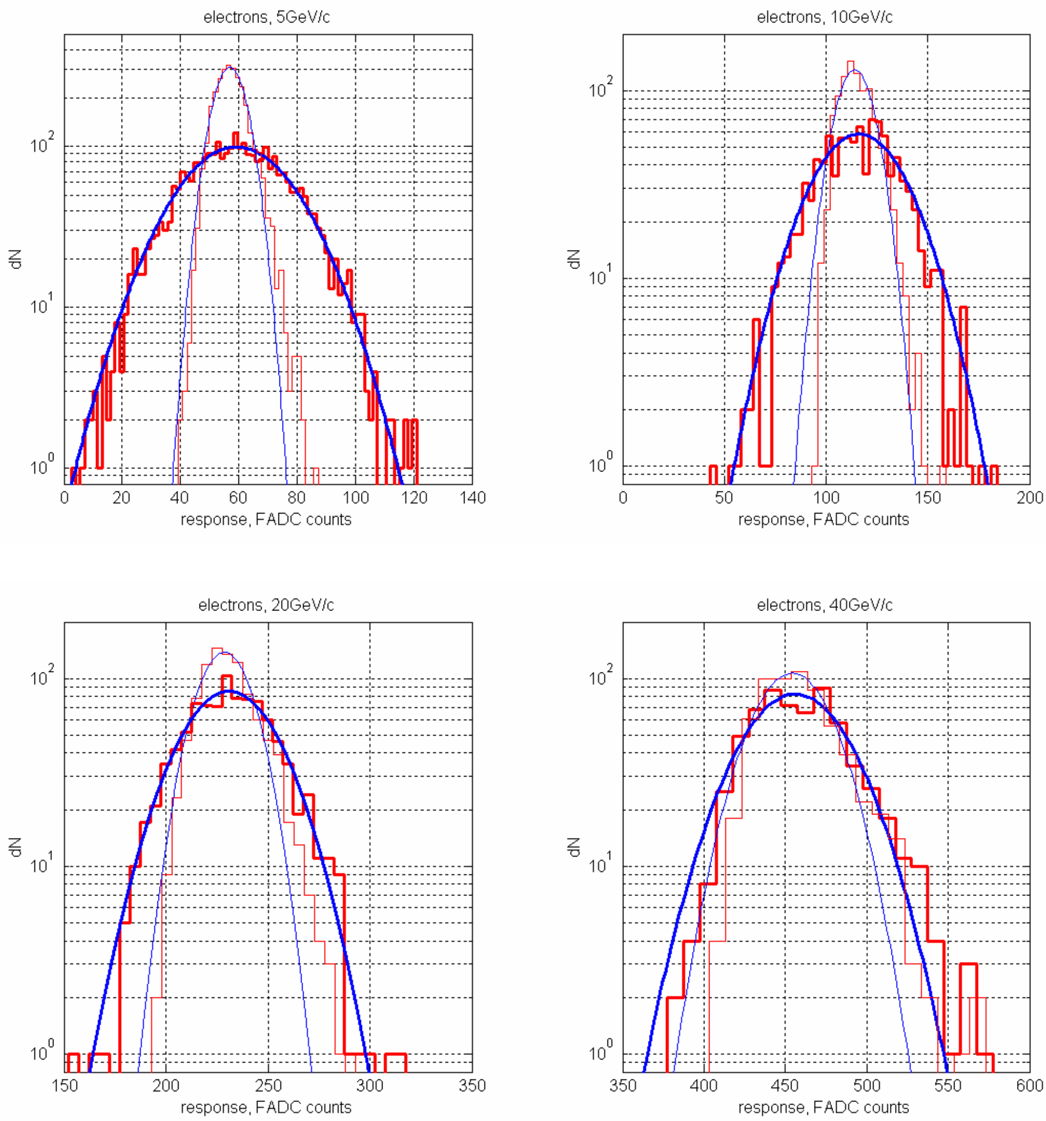

Figure 1.2: Distributions of the total signal from FCAL1: —— model data, —— Gaussian fit (thin lines: noise off; thick lines: noise on).

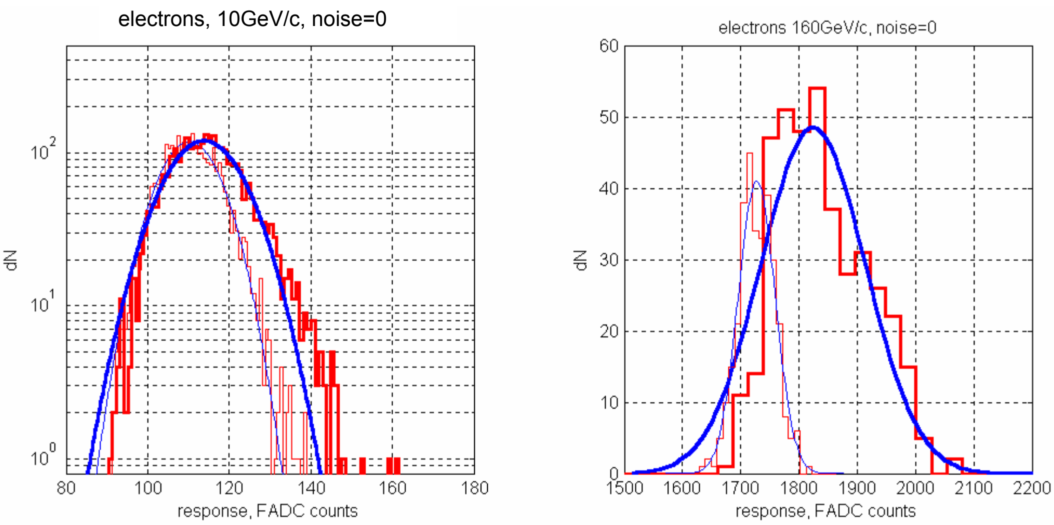

Figure 1.3: Distributions of the total signal from FCAL1, without noise: —— model data, —— Gaussan fit (thin lines: X=0, Y=0; thick lines: |X|≤3.5cm, |Y|≤3.5cm).

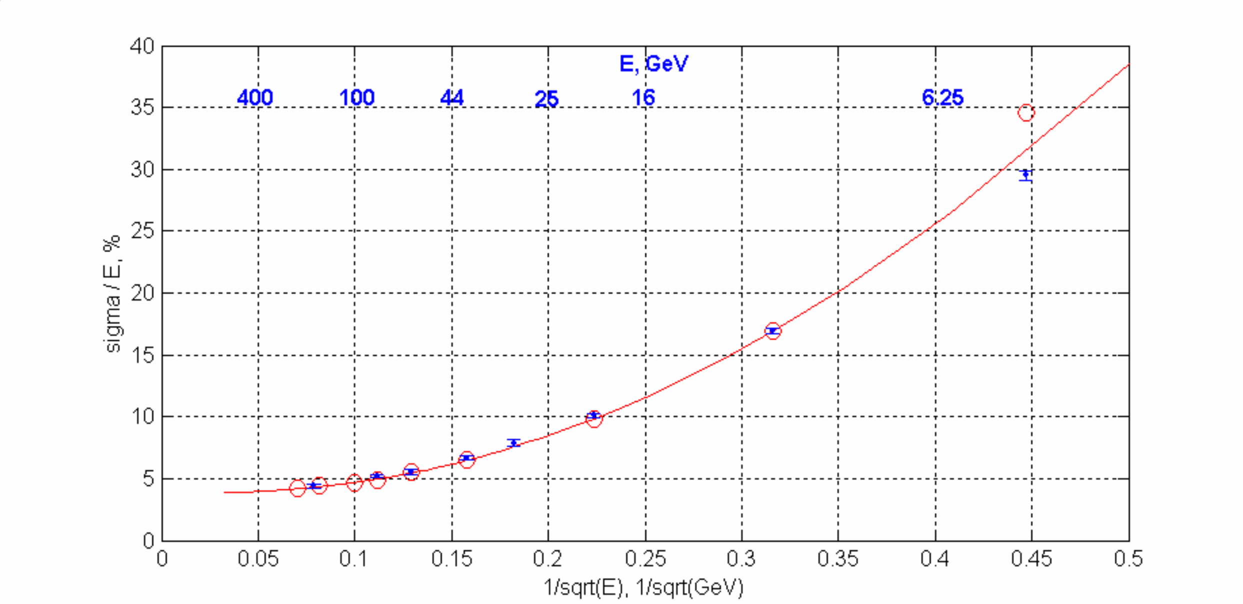

Figure 1.4: Energy dependence of the FCAL1 energy resolution on the energy

○ test 2003, ● MC model,

The line: fit of the data with the function $\frac{\sigma(E)}{E} = a \oplus \frac{b}{\sqrt{E}} \oplus \frac{c}{E}$

data 2003: a=(3.76±0.06)%, b=(24.5±0.84)%, c=(145.5±1.6)%

MC model: a=(3.67±0.26)%, b=(23.9±3.8)%, c=(140±6.3)%

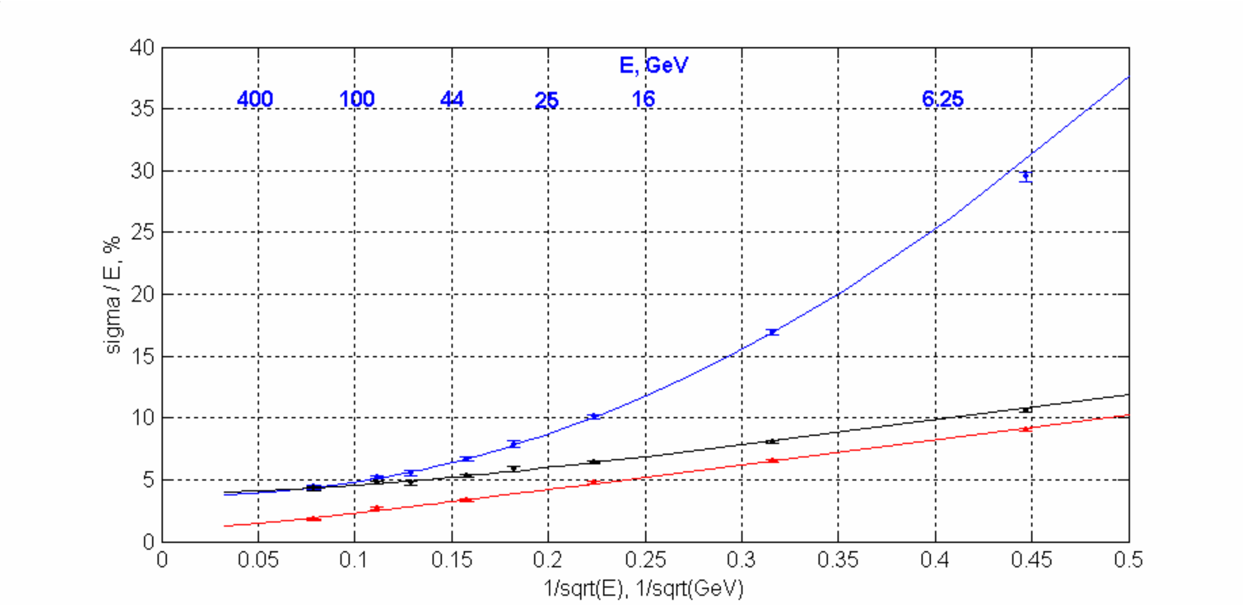

Figure 1.5: Energy dependence of the FCAL1 energy resolution on the energy (Monte-Carlo).

(noise off, X=0 Y=0), (noise off, |X, Y|≤3.5cm), (noise on, |X, Y|≤3.5cm)

The lines: fit of the data with the function $\frac{\sigma(E)}{E} = a \oplus \frac{b}{\sqrt{E}} \oplus \frac{c}{E}$ (with the noise on), or

$$\frac{\sigma(E)}{E} = a \oplus \frac{b}{\sqrt{E}}$$ (with the noise off).

MC (noise off, X=0 Y=0): a=(1.08±0.13)%, b=(20.3±0.2)%

MC (noise off, |X, Y|≤3.5cm): a=(3.96±0.10)%, b=(22.5±0.4)%

MC(noise on, |X, Y|≤3.5cm): a=(3.67±0.26)%, b=(23.9±3.8)%, c=(140±6.3)%

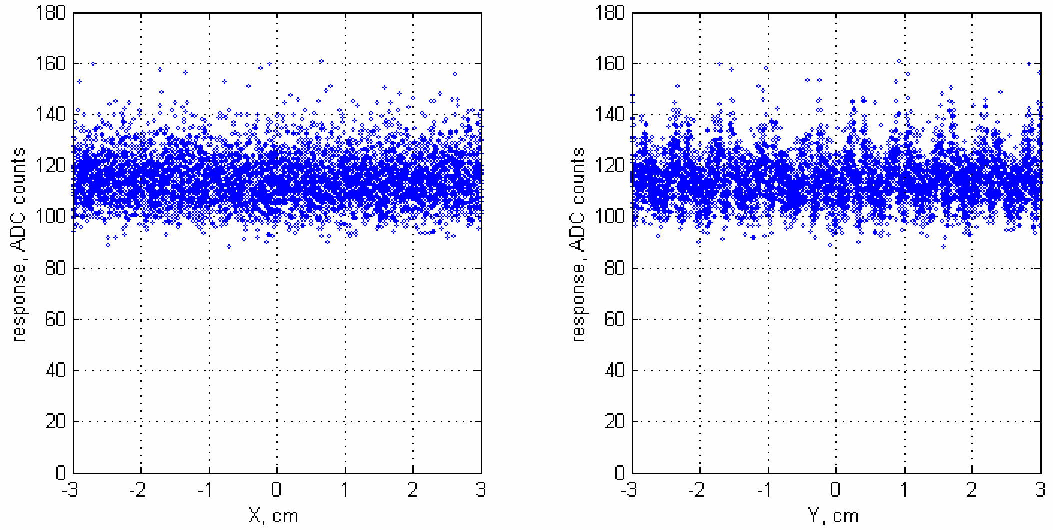

Figure 1.6: Simulated FCAL1 response vs. X and Y, 10 GeV/c, the model - noise off.